Malaysian Journal of Chemistry, 2022, Vol. 24(2), 37-46
(Special Issue: *2nd IKM Pahang Branch Symposium 2022 – Sustainability & Diversity Through Chemistry*)

One-Pot Sol-Gel Synthesis of a Zinc Oxide-Reduced Graphene Oxide Composite: Photocatalysis and Kinetics Studies using a Fuzzy Inference System

Zul Adlan Mohd Hir[1,2], Nik Muhammad Farhan Hakim Nik Badrul Alam[3], Ayu Sofia Shaari[1] and Hartini Ahmad Rafaie[4]*

[1]Faculty of Applied Sciences, Universiti Teknologi MARA Pahang,
26400 Bandar Tun Abdul Razak Jengka, Pahang, Malaysia
[2]Catalysis for Sustainable Water and Energy Nexus Research Group, School of Chemical Engineering,
College of Engineering, University Teknologi MARA, 40450 Shah Alam, Selangor, Malaysia
[3]Faculty of Computer and Mathematical Sciences, Universiti Teknologi MARA Pahang,
26400 Bandar Tun Abdul Razak Jengka, Pahang, Malaysia
[4] Faculty of Applied Sciences, Centre of Foundation Studies, Universiti Teknologi MARA,
Selangor Branch, Dengkil Campus, 43800 Dengkil, Selangor, Malaysia
*Corresponding author (e-mail: hartinirafaie@uitm.edu.my)

In this work, zinc oxide/reduced graphene oxide (ZnO/rGO) composites with different ratios synthesized by a one-pot sol-gel method were tested as photocatalysts for the degradation of methylene blue in aqueous solution. The physicochemical properties of the photocatalysts were characterised by FTIR and SEM-EDX. FTIR analysis showed the existence of various functional groups on the ZnO/rGO surfaces, which indicated strong interactions between the carbonyl, carboxylic, and hydroxyl groups on the rGO with ZnO particles. SEM images revealed a nearly spherical shape for ZnO which was homogeneously distributed on the rGO sheets, while the EDX results confirmed the presence of C, Zn, and O with increasing amounts of rGO. Based on a pseudo first-order kinetic model, the highest degradation rate constant, *k*, of 2.67×10^{-2} min^{-1} was obtained with 85% methylene blue degradation using a ZnO/rGO-10 photocatalyst. The relationship between the amount of rGO loadings, degradation percentage and rate constant was discussed using a fuzzy inference system (FIS). The introduction of a fuzzy logic controller (FLC) in this work provides the future direction and prediction for the creation of optimum ZnO/rGO photocatalysts for practical water recovery processes.

Key words: Fuzzy Inference System; photocatalysis; reduced graphene oxide; water recovery; zinc oxide

Received: December 2021; Accepted: February 2022

The infiltration of organic dye residues into the environment has generated a lot of attention in recent decades. It was reported that more than 50% of dye effluent was composed of azo dyes, which bear nitrogen π–bonds. Dyes generally have complex molecular structures that are light-stable and resistant to biodegradation, making them less likely to be easily decomposed [1]. Contamination of coloured wastewater not only brings toxic effects to humans and animals even at low concentrations, but also reduces light transmission in contaminated water, which in turn leads to oxygen starvation in aquatic life [2]

In a bid to curb the environmental accumulation of organic dye residues and their toxicity to land and aquatic biodiversity, semiconductor photocatalysis has been proposed as an efficient technology to combat such pollutants. In this regard, ZnO is typically employed for the removal of a wide range of organic contaminants as it is environmentally friendly, non-toxic, chemically stable, has a wide band gap (3.37 eV), and a greater quantum efficacy to absorb over a large fraction of the light spectrum (UV/solar) [3, 4]. Nonetheless, ZnO alone suffers from some technical aspects that hamper its performance, i.e., the inefficient separation of electron-hole pairs and a high sensitivity to photo-corrosion [5]. Therefore, there is a need to modify the surface properties of ZnO to enhance its photocatalytic performance.

Recently, two-dimensional carbon-based materials like sp^2 hybridized graphene have proved to be a good choice to modify ZnO and form heterostructures owing to their large surface area, outstanding electron mobility, and inhibition of direct charge recombination [6]. For instance, Ramesh et al. reported the use of reduced graphene oxide (rGO)-hybridized ZnO for the visible light

†Paper presented at the 2nd IKM Pahang Branch Symposium 2022 – Sustainability & Diversity Through Chemistry

photocatalytic degradation of Bisphenol A (BPA) [7]. The incorporated rGO significantly improved the BPA degradation efficiency by improving charge carrier migration and organic pollutant adsorption. Hu et al. studied the preparation of rGO-wrapped ZnO with improved degradation efficiency towards Rhodamine B dye [8]. Its outstanding performance may be attributed to the role of rGO, which acts as a charge separation enhancer and electron transport shuttle.

The present work investigated the synthesis of an ZnO/rGO photocatalyst via a facile one-pot sol-gel synthesis. Emphasis was placed on the effect of the formulation, physicochemical properties, and synergistic interaction between ZnO and rGO to facilitate the charge carrier transfer for the removal of methylene blue (MB) dye in the aqueous phase. A detailed study was also done to predict the photocatalytic performance using a fuzzy inference system (FIS), as to the best of our knowledge, the photocatalytic process of ZnO/rGO has never been studied. Thus, it was predicted that incorporating the ideal amount of rGO into ZnO, postulated by FIS modelling, could generate optimum photocatalytic performance for practical water recovery processes.

MATERIALS AND METHODS

Materials

Zinc nitrate hexahydrate ($Zn(NO_3)_2{\cdot}6H_2O$, 98%), methylene blue ($C_{16}H_{18}ClN_3S$, > 96%), sodium hydroxide (NaOH, > 97%), hexamethylenetetramine ($C_6H_{12}N_4$, > 99%), and reduced graphene oxide were supplied by Sigma-Aldrich (Selangor, Malaysia). All reagents were used as received, without purification. Deionized water was used throughout the experiments.

Preparation of ZnO/rGO Photocatalysts

The preparation of the ZnO/rGO photocatalysts was carried out by a facile one-pot sol-gel method. Zinc nitrate hexahydrate ($Zn(NO_3)_2{\cdot}6H_2O$) and hexamethylenetetramine ($C_6H_{12}N_4$) were dissolved in deionized water with continuous stirring at room temperature in a 500 mL beaker. The molar ratio of zinc nitrate hexahydrate to hexamethylenetetramine (Zn^{2+}: HMTA) was 1:1 to yield a 0.01 M slurry solution. Different amounts of rGO (7, 10 and 15 mg) were added to the slurry solutions at pH 10. After 1 h of continuous stirring, the resultant mixtures were sonicated at 50 °C for 30 min. The process was continued by heating the mixtures at 95 °C for 2 h to ensure homogeneity, before being left overnight for ageing. The precipitates were washed several times with deionized water and dried in an oven at 60 °C for 24 h followed by calcination at 500 °C for 1 h. For comparison purposes, pure ZnO was prepared using the same method but without addition of rGO.

Catalyst Characterizations

The functional groups of the prepared ZnO/rGO photocatalysts were analysed by Fourier transform infrared (FT-IR) between 400 to 4000 cm^{-1} on a Perkin Elmer infrared spectrometer using the attenuated total reflection (ATR) accessory. Their structural and elemental compositions were characterized using a scanning electron microscope equipped with an electron dispersive X-ray analyser (SEM- EDX, TESCAN VEGA3).

Evaluation of Photocatalytic Activity

The photodegradation of MB was carried out in a 250 mL beaker as shown in Figure 1. A known amount of prepared ZnO/rGO photocatalyst was suspended in a beaker containing 100 mL of 5 mg/L MB dye solution. The solution was stirred in the absence of light for 30 minutes to achieve the adsorption-desorption equilibrium. Next, the solution was exposed to UV-C light (λ = 254 nm) for 60 min with constant stirring. Samples of 5 ml were collected at 10 min intervals throughout the experiment. The concentration of MB in the solution was measured using a UV-vis Spectrophotometer (PerkinElmer Lambda 35) at λ_{max} = 664 nm, and the photodegradation percentage was evaluated using Equation 1.

$$\text{Degradation percentage (\%)} = (C_o - C_t)/C_o \times 100 \quad (1)$$

where C_o is the initial concentration of MB prior to irradiation and C_t is the concentration of MB after degradation at a specified time interval.

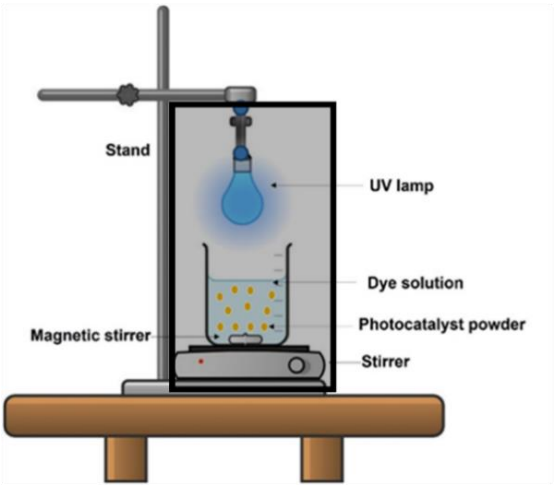

Figure 1. Schematic photodegradation measurement setup for degradation of methylene blue (MB) under UV irradiation

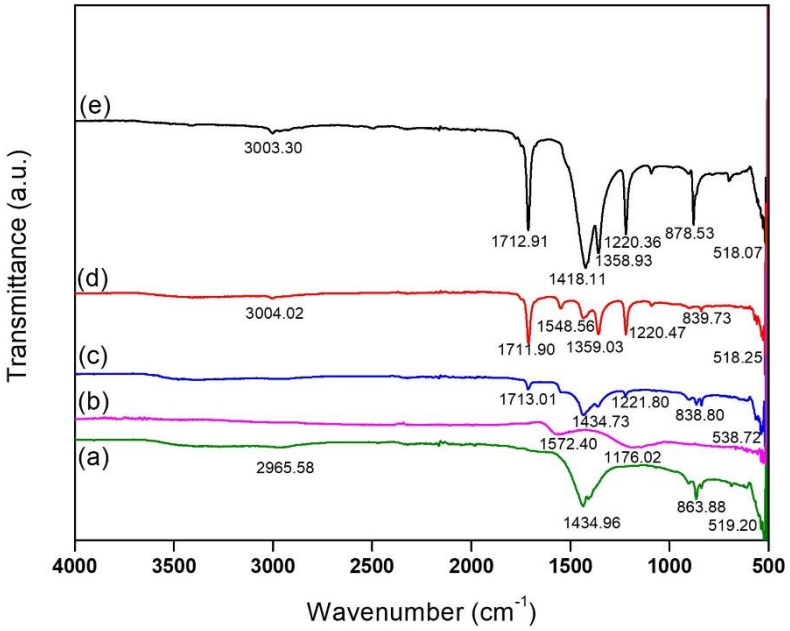

Figure 2. FTIR spectra of (a) pure ZnO, (b) rGO, (c) ZnO/rGO (7 mg), (d) ZnO/rGO (10 mg), and (e) ZnO/rGO (15 mg) composites

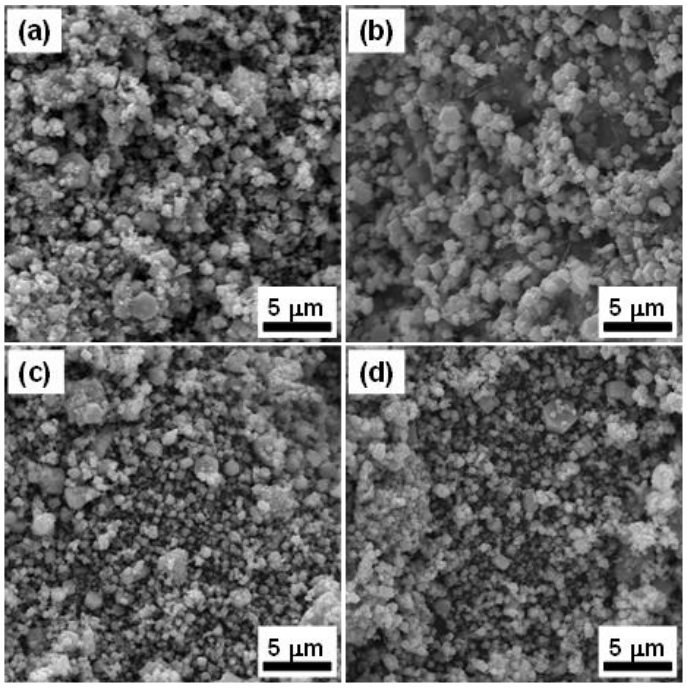

Figure 3. SEM images of (a) Pure ZnO, (b) ZnO/rGO (7 mg), (c) ZnO/rGO (10 mg), and (d) ZnO/rGO (15 mg) composites at 5000x magnification

RESULTS AND DISCUSSION

FTIR Analysis

Figure 2 displays the FTIR spectra of the prepared pure ZnO, rGO and ZnO/rGO composites after calcination at 500 °C for 1 h. At around 500–600 cm^{-1}, the peaks appear to be Zn–O stretching vibrations in all samples. The broad peak at 1572.40 cm^{-1} in the spectrum of rGO is due to to C=C, while the absorption peak at 1176.02 cm^{-1} is attributed to C-OH. In the case of the ZnO/rGO spectra, the peaks between

3000–3500 cm^{-1} and around 1700 $cm^{-1}$are assigned to –OH and C=O groups, the correlation of COOH moieties, respectively [9]. The peaks at around 1400, 1500, 1200, 800–1000 cm^{-1} correspond to the C–H, C=C, C–O–C (epoxy), and C–O (alkoxy) stretching vibrations, respectively [10, 11].

Surface Morphology and Elemental Composition

Figure 3 shows the surface morphology of the prepared pure ZnO and ZnO/rGO composites. The SEM image indicates that the pure ZnO microstructure is mostly spherical although some hexagonal shapes can also be seen in the micrograph (Figure 3a). All the ZnO/rGO composites were observed to have almost similar structures as ZnO was randomly dispersed on the rGO sheet (Figure 3b, c and d). The combination of rGO and ZnO is not clearly displayed in the micrographs as ZnO covered the entire rGO sheet. There was also no significant change in the particle size and shape of the prepared composites, and this might be due to the small amount of rGO being incorporated in the ZnO lattice. Figure 4 presents the elemental composition analysis of the prepared ZnO/rGO (10 mg) composites. The EDX analysis revealed the presence of C, Zn and O with no other peaks detected, confirming the purity of the samples. The existence of C confirmed that rGO was successfully incorporated into the ZnO samples. The mapping images show good dispersion of the particles. Elements are represented by red, green, and blue for Zn, O and C, respectively. The atomic percentage of C in the EDX analysis was observed to increase in parallel with the increase in rGO loading.

Photodegradation Activity of ZnO/rGO Photocatalyst

The photodegradation of MB by the prepared photocatalysts was measured using a UV-vis spectrophotometer and the results are presented in Figure 5. In the control experiment, the removal of MB was carried out in the dark for 30 min initially and subsequently for 60 min in the presence of photocatalysts and UV light. No photodegradation of MB was observed when the experiments were conducted under dark conditions. The photolysis of MB was also negligible, indicating its stability under UV light. The degradation percentage and rate increased in parallel with the increase in the amount of rGO up to 10 mg, which yielded the best degradation percentage of 85% (Figure 5a and b). The progressive degradation of MB was confirmed by the steady increase in the rate constant, *k* up to 2.67 $x10^{-2}$ min^{-1} before it decreased with the highest rGO loading (15 mg) (Figure 5c and d).

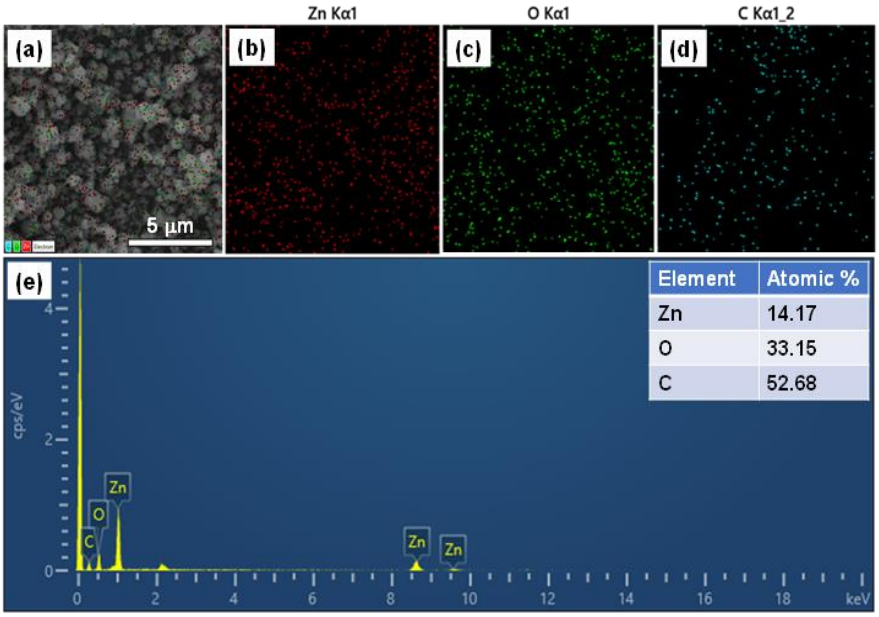

Figure 4. EDX analysis of (a) selected image of the ZnO/rGO (10 mg) composite, with corresponding elemental mapping images for Zn, O, and C presented in (b), (c), and (d), respectively, and (e) the elemental spectra and composition of the sample

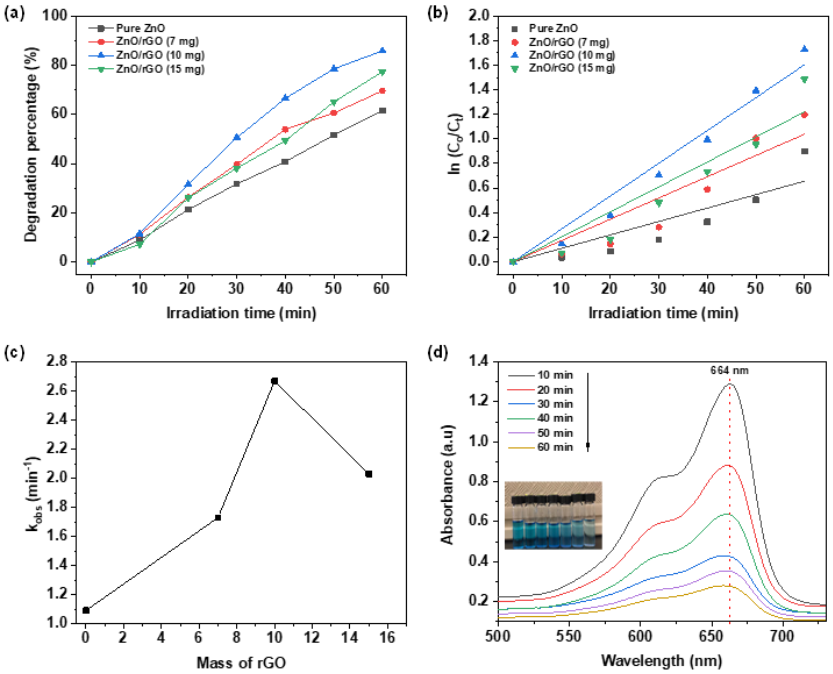

Figure 5. (a) Degradation percentage, (b) kinetics of the removal of MB by ZnO/GO composites with different rGO loadings (7–15 mg), (c) pseudo first-order rate constant, (d) UV-vis absorption spectra for ZnO/rGO (10 mg) composite

The photocatalytic enhancement is attributed to the strong and synergistic interaction between ZnO and rGO in which the rGO acts as an electron trapping site [12]. When ZnO receives the photon energy, the electrons (e^-) are excited from the valence band (VB) to the conduction band (CB), leaving positive holes (h^+) behind. These excited electrons then migrate from the CB of ZnO to the rGO sheet, subsequently avoiding recombination behaviour through effective separation of electron-hole pairs [13]. Thus, more charge carriers are produced with subsequent reactive oxidative species (•OH and $•O_2^-$) for efficient MB degradation (Figure 6). These radical species may be responsible for the degradation of MB. The holes can also degrade the MO molecules by directly reacting with them. However, both the degradation percentage and rate decrease significantly at a higher rGO loading (15 mg) due to particle agglomeration in the catalyst matrix, which reduces the surface area and light absorption capacity of the photocatalyst. This data shows that there is a limit to the amount of rGO that should be incorporated into the ZnO lattice (Table 1).

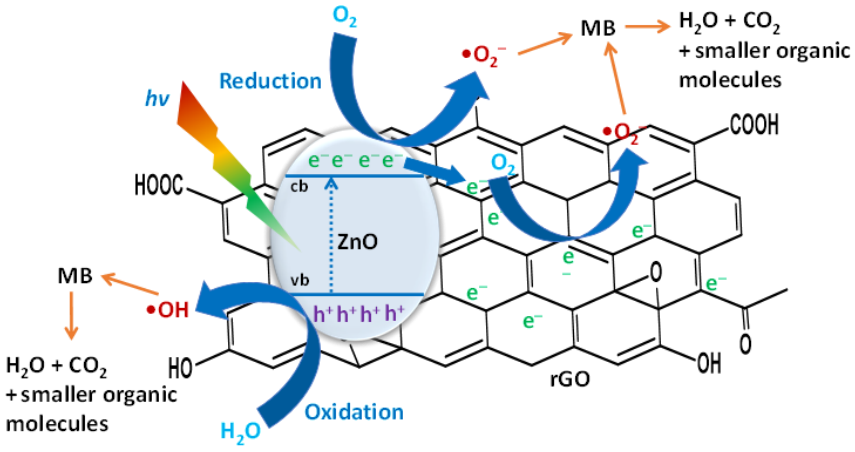

Figure 6. Plausible mechanism for the photodegradation of MB in the presence of ZnO/rGO composite photocatalysts under UV irradiation

Table 1. Photodegradation of MB using pure ZnO and ZnO/rGO composites with different rGO loadings

Sample	Degradation percentage (%)	Rate constant, k (min^{-1})	R^2 Value
Pure ZnO	61.60	1.09×10^{-2}	0.9021
ZnO/rGO (7 mg)	69.60	1.73×10^{-2}	0.9423
ZnO/rGO (10 mg)	85.86	2.67×10^{-2}	0.9890
ZnO/rGO (15 mg)	77.33	2.03×10^{-2}	0.9581

Table 2. Previous studies on photocatalytic degradation of MB using ZnO-graphene oxide

Composite	Degradation percentage (%)	Reaction time (min)	Reference
ZnO/GO	~98	90	[15]
ZnO/GO	99	140	[16]
ZnO/rGO/CNT	96	260	[17]
ZnO/rGO	88		
ZnO/rGO	85	60	This study

Table 2 lists previous reports on the photocatalytic reaction that employs ZnO-graphene oxide composites under UV light. This study showed that the synthesized composite with the optimum amount of rGO loading (10 mg) exhibited comparable photocatalytic degradation activity in comparison with previous research.

The Langmuir-Hinshelwood (L-H) kinetic model was used to examine the rate of MB degradation (Figure 5b), as expressed in the following equation [14].

$$r = \left(\frac{dC}{dt}\right) = k_{obs} \quad (2)$$

which can be rewritten as

$$\ln\left(\frac{C_0}{C_t}\right) = k_{obs}t \quad (3)$$

where k_{obs} represents the apparent pseudo-first-order rate constant obtained from the slope of the plot of $\ln (C_o/C_t)$ vs. irradiation time. C_o is the initial concentration, and C_t the concentration at a specified time interval (t).

PREDICTION USING A FUZZY INFERENCE SYSTEM

Fuzzy Inference System (FIS)

A fuzzy inference system (FIS) consists of a fuzzifier, an inference engine and a defuzzifier [18]. The fuzzifier converts data into fuzzy numbers, which are described in linguistic terms. Many types of fuzzy numbers have been used in the FIS, including triangular fuzzy numbers, trapezoidal fuzzy numbers, and Gaussian fuzzy numbers [19]. Each fuzzy number is characterized by a membership function, which represents the degree of belonging of the elements to the fuzzy set. Although any fuzzy number shape can be chosen to make up the FIS, Gaussian fuzzy numbers have shown applicability and adequacy in representing the uncertainty [20-22]. The Gaussian membership function is defined as follows:

$$\mu(x) = \frac{1}{\sqrt{2\pi\sigma}} \exp\left(-\frac{(x-m)^2}{2\sigma^2}\right) \quad (4)$$

where m and σ are the mean and standard deviation, respectively.

The inference engine consists of several rules in the form of "IF-THEN" to relate the fuzzified inputs with the corresponding outputs. Usually, experts in the field are required to create a set of IF-THEN rules to be used in the FIS. The defuzzifier converts the fuzzified outputs into crisp values. The FIS has been used in many applications such as hydrogen production activity [23], degradation of chlorhexidine digluconate [24] and degradation of tetracycline [25].

Prediction of Photocatalytic Activity

Predictions of the photocatalytic activity of pure ZnO and ZnO/rGO were made using the fuzzy command in MATLAB software. For this reason, a Mamdani fuzzy inference system was used with two input variables and two output variables, as shown in Figure 7.

The first input variable was doping with two linguistic terms: undoped ZnO and doped ZnO. The second input variable was the mass of rGO with five linguistic terms: very low, low, medium, high and very high. The membership functions of the input variables are presented in Figure 8 below.

To determine the performance of the photocatalytic activity, the percentage of degradation and the rate constant were considered as the output variables, as shown in Figure 9, in which five linguistic terms were used: very low, low, moderate, high and very high.

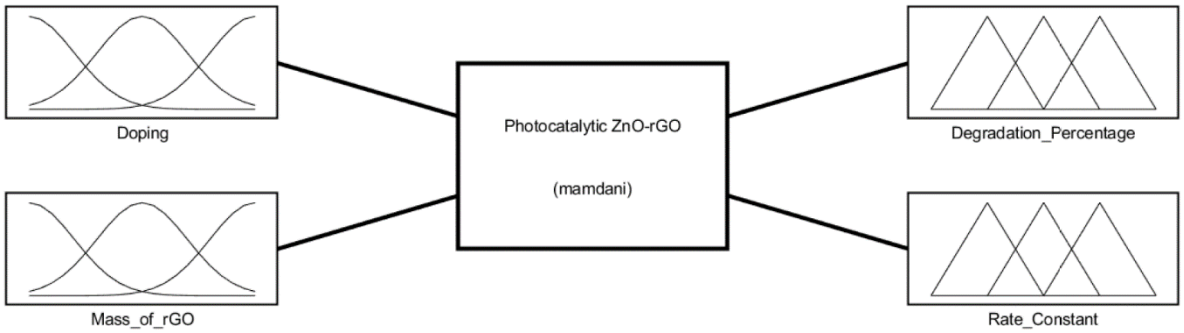

Figure 7. A Mamdani inference system for predicting photocatalytic activity

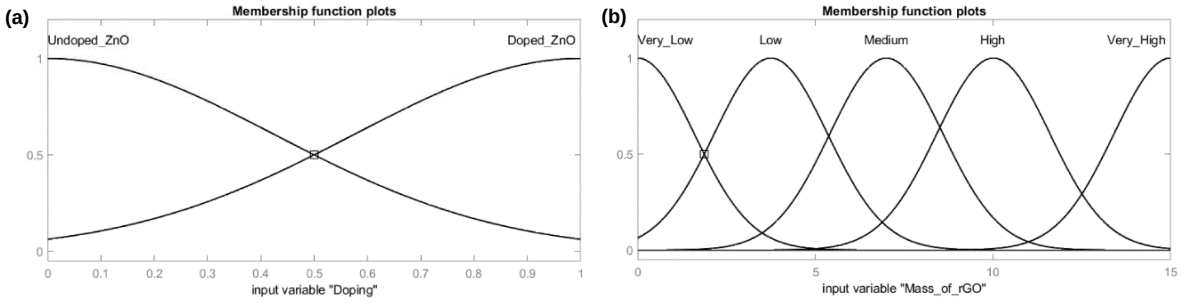

Figure 8. Membership functions of input variables: (a) doping, (b) mass of Rgo

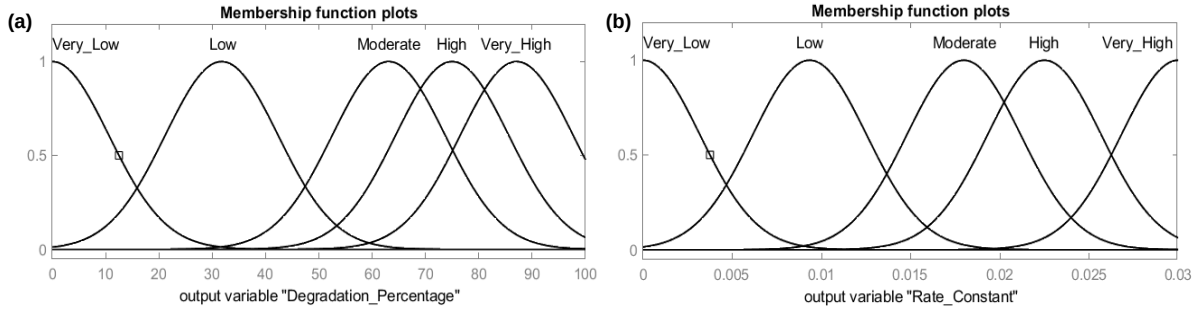

Figure 9. Membership functions of output variables: (a) degradation percentage, (b) rate constant

In relating the input and output variables, six IF-THEN rules were defined as follows:

1. If (Doping is Undoped ZnO), then (Degradation Percentage is Moderate) (Rate Constant is Low).
2. If (Doping is Doped ZnO) and (Mass of rGO is Very Low), then (Degradation Percentage is Moderate)(Rate Constant is Low).
3. If (Doping is Doped ZnO) and (Mass of rGO is Low), then (Degradation Percentage is Moderate)(Rate Constant is Low).
4. If (Doping is Doped ZnO) and (Mass of rGO is Medium), then (Degradation Percentage is Moderate) (Rate Constant is Moderate).
5. If (Doping is Doped ZnO) and (Mass of rGO is High), then (Degradation Percentage is Very High) (Rate Constant is Very High).
6. If (Doping is Doped ZnO) and (Mass of rGO is Very High), then (Degradation Percentage is High)(Rate Constant is High).

Figure 10 shows the curves obtained with the proposed FIS model, which defined the relations between the input variables and each of the output variables. The graphs relate the mass of rGO with the percentage of degradation and rate constant. The degradation percentage was low in parallel with the low mass of rGO, but then increased when the mass of rGO was greater than 5.2 mg. The highest degradation percentage was obtained when the mass of rGO reached 10.7 mg; however, the percentage performance dropped when the mass of rGO exceeded 10.9 mg. The rate constant increased with the increasing mass of rGO. The maximum rate constant was obtained when 10.7 to 11.0 mg of rGO was used. The rate constant dropped when the mass exceeded 11.0 mg, showing a similar pattern to the degradation percentage. After analysing the graphs, the ideal mass of rGO for optimal photocatalytic activity was found to be in the range of 10.7 mg to 10.9 mg.

CONCLUSION

ZnO/rGO composite photocatalysts were successfully prepared by incorporating rGO at different loadings via a simple one-pot sol-gel method. FTIR analysis indicated the presence of several functional groups which were assigned to their respective stretching vibrations, namely Zn–O (500–600 cm^{-1}), –OH (3000–3500 cm^{-1}), and C=O (1700 cm^{-1}) in relation to the COOH moieties. The highest degradation percentage of 85% was obtained using ZnO/rGO (10 mg) to degrade 5 mg/L of MB solution, which outperformed pure ZnO and its counterparts. The degradation rate, k, reached the highest at 2.67×10^{-2} within 60 min of reaction time. This can be explained in terms of improving the lifetime of the electron-hole pairs due to the trapping of electrons promoted by the presence of rGO, which provided electron trapping sites to avoid recombination. The use of a fuzzy inference system (FIS) was able to determine the ideal mass of rGO needed for optimal photocatalytic activity. In this study, the limitation on the number of

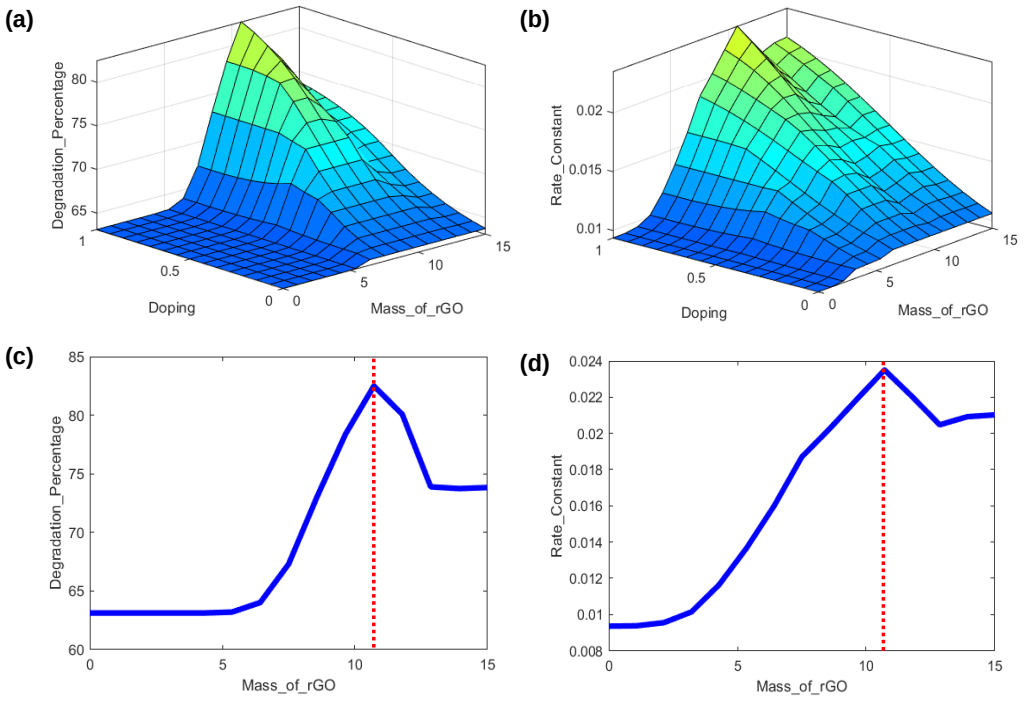

Figure 10. Curves obtained using the proposed FIS model, (a) & (c): prediction of degradation percentage, (b) & (d): prediction of rate constant

input variables caused fewer IF-THEN rules to be generated in the FIS. In future, other input variables such as initial dye concentration, catalyst loading, irritation time, and different types of irradiation may also be considered.

ACKNOWLEDGMENT

The authors gratefully acknowledge the Ministry of Higher Education (MOHE) and Universiti Teknologi MARA (UiTM) for the FRGS-RACER (600-RMI/FRGS/RACER 5/3 (041/2019)) and YTR (600-RMC/YTR/5/3 (005/2020)) grants, as well as the services and facilities provided by UiTM Pahang Branch to carry out the laboratory work.

The authors declare that they have no conflict of interest.

REFERENCES

1. Serrà, A., Philippe, L., Perreault, F. and Garcia-Segura, S. (2021) Photocatalytic treatment of natural waters. Reality or hype? The case of cyanotoxins remediation. *Water Res.*, **188**, 116543.

2. Briffa, J., Sinagra, E. and Blundell, R. (2020) Heavy metal pollution in the environment and their toxicological effects on humans. *Heliyon*, **6(9)**, e04691.

3. Hir, Z. A. M., Abdullah, A. H., Zainal, Z. and Lim, H. N. (2017) Photoactive Hybrid Film Photocatalyst of Polyethersulfone-ZnO for the Degradation of Methyl Orange Dye: Kinetic Study and Operational Parameters. *Catalysts*, **7(11)**, 313.

4. Weldegebrieal, G. K. (2020) Synthesis method, antibacterial and photocatalytic activity of ZnO nanoparticles for azo dyes in wastewater treatment: A review. *Inorg. Chem. Commun.*, **120**, 108140.

5. Uribe-López, M. C., Hidalgo-López, M. C., López-González, R., Frías-Márquez, D. M., Núñez-Nogueira, G., Hernández-Castillo, D. and Alvarez-Lemus, M. A. (2021) Photocatalytic activity of ZnO nanoparticles and the role of the synthesis method on their physical and chemical properties. *J. Photochem. and Photobiol. A: Chemistry*, **404**, 112866.

6. Landström, A., Gradone, A., Mazzaro, R., Morandi, V. and Concina, I. (2021) Reduced graphene oxide-ZnO hybrid composites as photocatalysts: The role of nature of the molecular target in catalytic performance. *Ceram. Int.*, **47**, 19346–19355.

7. Ramesh, K., Gnanavel, B. and Shkir, M. (2021) Enhanced visible light photocatalytic degradation of bisphenol A (BPA) by reduced graphene oxide (RGO)–metal oxide (TiO_2, ZnO and WO_3) based nanocomposites. *Diam. Relat. Mater.*, **118**, 108514.

8. Hu, W. C., Chen, Y. A., Hsieh, P. Y., Tsao, C. W., Chiu, Y. H., Chang, T. F. M., Chen, C. Y., Sone, M. and Hsu, Y. J. (2020) Reduced graphene oxides-wrapped ZnO with notable photocatalytic property. *J. Taiwan Inst. Chem. Eng.*, **112**, 337–344.

9. Chen, D., Wang, D., Ge, Q., Ping, G., Fan, M., Qin, L., Bai, L., Lv, C. and Shu, K. (2015) Graphene-wrapped ZnO nanospheres as a photocatalyst for high performance photocatalysis. *Thin Solid Films*, **574**, 1–9.

10. Kumar, S., Pandit, V., Bhattacharyya, K. and Krishnan, V. (2018) Sunlight driven photo-catalytic reduction of 4-nitrophenol on Pt decorated ZnO-RGO nanohetero-structures. *Mater. Chem. Phys.*, **214**, 364–376.

11. Elumalai, N., Prabhu, S., Selvaraj, M., Silambarasan, A., Navaneethan, M., Harish, S., Ramu, P. and Ramesh, R. (2021) Enhanced photocatalytic activity of ZnO hexagonal tube/rGO composite on degradation of organic aqueous pollutant and study of charge transport properties. *Chemosphere*, **132782**.

12. Julkapli, N. M. and Bagheri, S. (2014) Graphene supported heterogeneous catalysts: An overview. *Int. J. Hydrogen Energy*, **40**, 948–979.

13. Rafaie, H. A., Nor, R. M., Azmina, M. S., Ramli, N. I. T. and Mohamed, R. (2017) Decoration of ZnO microstructures with Ag nanoparticles enhanced the catalytic photodegradation of methylene blue dye. *J. Environ. Chem. Eng.*, **5**, 3963–3972.

14. Chijioke-Okere, M. O., Hir, Z. A. M., Ogukwe, C. E., Njoku, P. C., Abdullah, A. H. and Oguzie, E. E. (2021) TiO_2/Polyethersulphone films for photocatalytic degradation of acetaminophen in aqueous solution. *J. Mol. Liq.*, **338**, 116692.

15. Lin, Y., Hong, R., Chen, H., Zhang, D. and Xu, J. (2020) Green Synthesis of ZnO-GO Composites for the Photocatalytic Degradation of Methylene Blue. *J. Nanomaterials*, **4147357**.

16. Hosseini, S. A. and Babaei, S. (2017) Graphene Oxide/Zinc Oxide (GO/ZnO) Nanocomposite as a Superior Photocatalyst for Degradation of Methylene Blue (MB)-Process Modeling by

Response Surface Methodology (RSM), *J. Braz. Chem. Soc*., **28(2)**, 299–307.

17. Lv, T., Pan, L., Liu, X. and Sun, Z. (2012) Enhanced photocatalytic degradation of methylene blue by ZnO–reduced graphene oxide–carbon nanotube composites synthesized via microwave-assisted reaction, *Catal. Sci. Technol*., **2**, 2297–2301.

18. Wang, K. (2001) Computational intelligence in agile manufacturing engineering: *Agile Manufacturing The 21st Century Competitive Strategy*, Elsevier Science Ltd: Oxford, UK.

19. Pieczynski, A. (2002) Fuzzy modeling of multi-dimensional non-linear process–influence of membership function shape. *Proc. 8th East West Zittau Fuzzy Colloquium*, 125–133.

20. Pieczyński, A. and Obuchowicz, A. (2004) Application of the general Gaussian membership function for the fuzzy model parameters tunning. *International Conference on Artificial Intelligence and Soft Computing*, *Berlin*, 350–355.

21. Kreinovich, V., Quintana, C. and Reznik, L. (1992) Gaussian membership functions are most adequate in representing uncertainty in measurements. *Proceedings of NAFIPS*, **92**, 15–17.

22. Yılmaz, M. and Arslan, E. (2008) Effect of the type of membership function on geoid height modelling with fuzzy logic. *Survey Review*, **40(310)**, 379–391.

23. Ibrahim, N. S., Leaw, W. L., Mohamad, D., Alias, S. H. and Nur, H. (2020) A critical review of metal-doped TiO2 and its structure–physical properties–photocatalytic activity relationship in hydrogen production. *International Journal of Hydrogen Energy*, **45(53)**, 28553–28565.

24. Sarkar, S., Chowdhury, R., Das, R., Chakraborty, S., Choi, H. and Bhattacharjee, C. (2014) Application of ANFIS model to optimise the photocatalytic degradation of chlorhexidine digluconate. *RSC Advances*, **4(40)**, 21141–21150.

25. Tabatabai-Yazdi, F. S., Pirbazari, A. E., Saraei, F. E. K. and Gilani, N. (2021) Construction of graphene based photocatalysts for photocatalytic degradation of organic pollutant and modeling using artificial intelligence techniques. *Physica B: Condensed Matter*, **608**, 412869.